

Cortico-muscular coherence and brain networks in familial adult myoclonic epilepsy and progressive myoclonic epilepsy

Silvana Franceschetti ^{a,*}, Elisa Visani ^b, Ferruccio Panzica ^c, Antonietta Coppola ^d, Pasquale Striano ^{e,f}, Laura Canafoglia ^g

^a Neurophysiopathology, Fondazione IRCCS Istituto Neurologico Carlo Besta, Milan, Italy

^b Bioengineering Unit, Dept. of Diagnostic and Technology, Fondazione IRCCS Istituto Neurologico Carlo Besta, Milan, Italy

^c Clinical Engineering, Fondazione IRCCS Istituto Neurologico Carlo Besta, Milan, Italy

^d Department of Neuroscience, Odontostomatology and Reproductive Sciences, Federico II, University of Naples, Napoli, Italy

^e IRCCS Istituto "Giannina Gaslini", Genova, Italy

^f Department of Neurosciences, Rehabilitation, Ophthalmology, Genetics, Maternal and Child Health, University of Genova, Genova, Italy

^g Integrated Diagnostics for Epilepsy, Dept of Diagnostic and Technology, Fondazione IRCCS Istituto Neurologico Carlo Besta, Milan, Italy

HIGHLIGHTS

- FAME2, compared to EPM1, had confined beta-cortico-muscular coherence (CMC) and increased centrality index in the sensorimotor region contralateral to movement.
- In FAME2, CMC distribution and increased centrality index could counteract the severity and the spreading of the myoclonus.
- In FAME2, there was a main decline in the network connectivity indexes, possibly linked to neuropsychological comorbidities.

ARTICLE INFO

Article history:
Accepted 24 April 2023
Available online

Keywords:
Cortico-muscular coherence
Network connectivity
FAME2
EPM1
Betweenness centrality
Global Efficiency

ABSTRACT

Objective: Familial Adult Myoclonic Epilepsy (FAME) presents with action-activated myoclonus, often associated with epilepsy, sharing various features with Progressive Myoclonic Epilepsy (PMEs), but with slower course and limited motor disability. We aimed our study to identify measures suitable to explain the different severity of FAME2 compared to EPM1, the most common PME, and to detect the signature of the distinctive brain networks.

Methods: We analyzed the EEG-EMG coherence (CMC) during segmental motor activity and indexes of connectivity in the two patient groups, and in healthy subjects (HS). We also investigated the regional and global properties of the network.

Results: In FAME2, differently from EPM1, we found a well-localized distribution of beta-CMC and increased betweenness-centrality (BC) on the sensorimotor region contralateral to the activated hand.

In both patient groups, compared to HS, there was a decline in the network connectivity indexes in the beta and gamma band, which was more obvious in FAME2.

Conclusions: In FAME2, better localized CMC and increased BC in comparison with EPM1 patients could counteract the severity and the spreading of the myoclonus.

Decreased indexes of cortical integration were more severe in FAME2.

Significance: Our measures correlated with different motor disabilities and identified distinctive brain network impairments.

© 2023 International Federation of Clinical Neurophysiology. Published by Elsevier B.V. All rights reserved.

Abbreviations: FAME, Familial Adult Myoclonic Epilepsy; PME, Progressive Myoclonic Epilepsy; CMC, Cortico-muscular coherence; BC, Betweenness-centrality; EGlob, Global efficiency.

* Corresponding author at: Neurophysiopathology, Fondazione IRCCS Istituto Neurologico Carlo Besta, Via Celoria 11, 20133 Milan, Italy.

E-mail addresses: silvana.franceschetti@istituto-besta.it (S. Franceschetti), elisa.visani@istituto-besta.it (E. Visani), ferruccio.panzica@istituto-besta.it (F. Panzica), laura.canafoglia@istituto-besta.it (L. Canafoglia).

<https://doi.org/10.1016/j.clinph.2023.04.009>

1388-2457/© 2023 International Federation of Clinical Neurophysiology. Published by Elsevier B.V. All rights reserved.

1. Introduction

Familial Adult Myoclonic Epilepsy, with dominant inheritance (FAME), presents as an adolescent/adult-onset myoclonus often associated with epilepsy. The movement disorder was originally described as “cortical tremor”, as a variant of cortical reflex myoclonus (Ikeda et al., 1990), associated with cortical spikes (Oguni

et al., 1995; Terada et al. 1997). Electrophysiological studies revealed signs of sensorimotor cortical hyperexcitability, further indicating a cortical origin, including giant somatosensory evoked potentials (SEPs), enhanced long-loop C-reflexes, increased facilitation, and decreased inhibition in response to transcranial magnetic stimulation (Oguni et al., 1995; Cen et al., 2016; Tojima et al., 2021; Dubbioso et al., 2022). Moreover, some data suggested the involvement of a cerebellar-thalamocortical loop in the pathophysiology of FAME (Latorre et al., 2020; Wang et al., 2022).

Several patients also have seizures and show generalized spike and wave complexes on EEG, and sometimes photo-paroxysmal responses (Terada et al., 1997; Cen et al., 2016).

Expanded TTCA and TTTA in an intronic region of different genes in different ethnical groups are the causative factors (Ishiura et al., 2018; Corbett et al., 2019; Florian et al., 2019; Yeetong et al., 2019), all patients are included in the FAME category, with similar even if non-identical phenotypes. Among them, FAME2 (MIM #607876) has been reported in adults, with relatively late onset of rhythmic myoclonic jerks, sometimes associated with seizures, photosensitivity, possible cognitive decline, and frequent psychiatric symptoms (Guerrini et al., 2001; Crompton et al., 2012; Licchetta et al., 2013; Coppola et al., 2016; Kobayashi et al., 2018).

We included in our study 13 patients with genetically confirmed FAME2, from two families (n. 2 and 22 reported by Corbett et al., 2019), all showing a limited motor disability, and we evaluated the cortico-muscular coherence (CMC) and network indexes based on EEG-EMG polygraphic recordings.

To understand why cortical myoclonus is much less severe in FAME2 patients than in patients with typical progressive myoclonic epilepsy (PME), we evaluated measures obtained from polygraphic recordings performed in patients with FAME2 and compared them with those obtained from 13 patients with Unverricht-Lundborg disease (EPM1 #254800). In particular, we estimated the cortico-muscular coherence (CMC) and indexes derived from graph analysis capable of providing information on the cortical network in the two patient populations. Taking into account the different courses of the disease in the two groups of patients, we chose patients with EPM1 as this form is less severe than many other PMEs and tends to reach relative stability in adulthood (Ramachandran et al., 2009).

2. Methods

2.1. Patients

We included 13 patients with a molecular diagnosis of FAME2 (5-bp repeat expansion, ATTC, in intron 1 of the *STARD7* gene (#616712) in chromosome 2q11 (four females; age 55.3 ± 4.2 years). Moreover, we included 13 patients with “mild” EPM1 (#254800; all carrying homozygous CCC-CGC-CCC-GCG dodecamer repeat expansions on chromosome 21q22 at the promoter of cystatin B gene (9 females; age 44.5 ± 2.7 years), with prominent myoclonus, not associated with important cerebellar signs, cognitive impairment, or recurrent seizures (Kälviäinen et al., 2008; Canafoglia et al., 2017). The age of the two patient groups had a weakly significant statistical difference ($t(24) = 2.1, p = 0.046$). Moreover, we compared these two groups with 11 healthy subjects (HS, 5 females; age 43.3 ± 4.1 years). All patients and HS were right-handed and able to collaborate on the polygraphic recording and requested motor tasks.

All EPM1 patients received anti-seizure medications (ASM), as reported in Table 1, and all had very few seizures at the disease onset. Seven of the 13 FAME2 patients had occasional seizures in the past and received chronic ASM (one had infantile-onset sei-

zures reported as “spasms”; then he developed focal to bilateral seizures).

According to the simplified myoclonus score (Magaudda et al., 2004), the EPM1 patients had a myoclonus score ranging from two to five, while FAME2 patients had scores from one to three (Table 1).

At the time of this evaluation, all patients had EEG abnormalities absent or limited to occasional residual diffuse brief spike-wave sequences. All EPM1 patients had PPR during the initial stage of the disease, which persisted in two of them at the time of this evaluation. “Subclinical” PPR was present also in four FAME2 and in two EPM1 patients.

Somatosensory evoked potentials (SEPs) and C-reflex data were available for all EPM1 and for 11 of the 13 FAME2 patients. SEPs were elicited by electrically stimulating the median nerve at the wrist at an intensity that was just over the motor threshold with a stimulation frequency of 1 Hz. SEPs were defined as “giant” when the amplitudes of N20P25 and P25N33 cortical components exceeded the mean value + 3SD the normative laboratory values ($12.3 \mu\text{V}$ and $8.6 \mu\text{V}$ for N20P25 and P25N33 respectively; Visani et al., 2013). C-reflex was obtained in all EPM1 and in nine FAME2 patients, using surface electrodes positioned on the thenar muscle and evoked by electrical stimulation at the wrist just over the motor threshold at a frequency rate of 0.5 Hz.

The study was approved by the Ethics Committee of the Fondazione IRCCS Istituto Neurologico Carlo Besta and carried out according to the Declaration of Helsinki, and its amendments. All of the subjects gave their written informed consent before being included in the study.

2.2. EEG-polygraphic recordings

We evaluated the EEG-polygraphic recordings from 19 scalp electrodes positioned according to the International 10–20 system with reference to linked earlobes and EMG from surface electrodes positioned in all patients on various muscles always including bilateral wrist extensor and flexor.

The sampling frequency was set at 512 Hz and the EEG signals were band-pass filtered in the range of 1.6–120 Hz. We evaluated the EEG at rest and during maintained unilateral isometric wrist extension.

Two epochs lasting 30 seconds of EEG and EMG signals obtained at the onset of right-hand extension and free from artifacts, were selected for the analyses. We also analyzed epochs of equal duration recorded under resting conditions. Taking into account the preliminary examination done on individual electrodes, we grouped the electrodes in different regions of interest (ROIs). We defined the following ROIs: L sensorimotor (L-SM) as the mean of the values measured on F3, C3, and P3, R sensorimotor (R-SM) as the mean of F4, C4, and P4 values, vertex region (V) as the mean of Fz, Cz, Pz values. We never found a significant difference in values obtained from left and right frontopolar (FP) or occipital (OCC) electrodes; therefore, we included as FP values the mean of the values of Fp1 and Fp2 and as occipital (OCC) ROI the mean of the values of O2 and O1.

2.3. Power spectrum density and cortico-muscular coherence analysis

We estimated the power spectrum density (PSD) at rest and CMC during isometric contraction using a blockwise autoregressive parametric model (AR, Panzica et al., 2003); the model order was determined using the multichannel version of the Akaike criterion, while we used a ‘portmanteau’ chi-square and Anderson’s tests to verify the goodness of the identification. We evaluated both PSD and CMC in delta (1–4 Hz), theta (4–8 Hz), alpha (8–13 Hz), beta (13–30 Hz), and low gamma (30–40 Hz) bands.

Table 1

Main demographic and clinical data of FAME2 and EPM1 patients. TC = tonic-clonic seizures, myo = myoclonic seizures, F = focal seizures, VPA = valproate, BZ = benzodiazepines (clonazepam or diazepam), PRM = primidone, LEV = levetiracetam, PER = perampanel, GBT = vigabatrin, SRT = sertraline, PAR = paroxetine, ZON = zonisamide, TPM = topiramate, PB = phenobarbital.

	Age (ys)	Onset (ys)	Disease duration (ys)	Score	Seizures type	Seizure free	PPR	ASMs
FAME2 1	34	18	16	2	TC	yes	no	PRM
FAME2 2	39	14	25	2	no	yes	no	-
FAME2 3	49	20	29	2	no	yes	yes	-
FAME2 4	49	15	34	3	TC	yes	no	PRM, LEV
FAME2 5	49	20	34	2	no	yes	no	-
FAME2 6	70	20	50	3	TC	yes	yes	PRM,VPA, PER, BZ
FAME2 7	36	20	16	1	no	yes	no	-
FAME2 8	78	23	55	2	no	yes	no	-
FAME2 9	78	40	38	3	Visual, TC	Yes	no	VPA, PB
FAME2 10	57	41	16	2	no	yes	yes	VPA
FAME2 11	64	30	34	2	TC	yes	yes	BZ, PAR
FAME2 12	70	40	30	2	TC	yes	no	GBT, SRT
FAME2 13	65	54	11	3	Spasms (2 ys)	yes	no	VPA
EPM1 1	32	12	20	2	TC & myo	yes	no	VPA, BZ
EPM1 2	32	9	23	2	TC & myo	yes	yes	VPA
EPM1 3	46	16	30	3	TC & myo	yes	yes	VPA, BZ, PRM, LEV
EPM1 4	48	9	39	3	TC & myo	yes	no	VPA, PB, BZ
EPM1 5	48	11	37	4	TC & myo	yes	no	VPA,CLZ, LEV
EPM1 6	36	11	25	3	TC & myo	yes	no	VPA, LEV
EPM1 7	48	11	37	5	TC & myo	yes	no	PB, BZ, VPA, TPM, LEV
EPM1 8	48	12	36	5	TC & myo	yes	no	VPA, BZ, TPM
EPM1 9	56	12	44	5	TC & myo	yes	no	PB, VPA, BZ
EPM1 10	56	11	45	5	TC & myo	yes	no	VPA, BZ
EPM1 11	65	10	55	5	TC & myo	yes	no	LEV, VPA, TPM, BZ
EPM1 12	38	12	26	4	TC & myo	yes	no	VPA, BZ
EPM1 13	38	12	26	3	TC & myo	yes	no	VPA, PER, ZON

2.4. Network analysis

Generalized partial directed coherence (gPDC, [Baccalà et al., 2013](#)), and indexes derived from graph theory-based measures were estimated on the same epochs and in the same frequency bands used for rest and CMC analyses.

The gPDC was applied to estimate the directional flow of information between pairs of signals, with values ranging from 0 (no connectivity) to 1 (maximal connectivity). We assessed the statistical significance of non-zero values at each frequency by a bootstrap approach using phase randomization, based on Theiler's method ([Theiler, 1992](#); [Zoubir and Iskander, 2004](#)).

To investigate the regional properties of the network, we calculated the in- and out-degrees (the number of edges going into or going out of a node, considering each ROI as a node). Moreover, we calculated the betweenness-centrality (BC), measuring the centrality in a graph of a specific region based on shortest paths, and the clustering coefficient (CC), measuring the degree to which a network organizes into a region. We also evaluated as indexes of the whole brain network the global efficiency (EGlob), measuring the capacity for parallel information transfer, and the characteristic path length (CPL), giving the average number of edges in the shortest paths between all node pairs, in the different frequency bands.

The signals were pre-processed and analyzed using a custom-written toolbox in MATLAB (MathWorks Inc., Natick, MA, U.S.A.) containing modified functions from Biosig ([Vidaurre et al., 2011](#)) and ARFit ([Schneider and Neumaier, 2001](#)) toolboxes.

2.5. Statistical analysis

We applied repeated measures analysis of variance (RM-ANOVA) at a significance level of 5% to PSD relative power, CMC values, and connectivity indexes using groups (HS, EPM1, FAME2) as between factor and ROIs as within-subject factors. The sphericity assumption was evaluated using Mauchly's test, and, in the case of its violation, the Greenhouse-Geisser correction was applied.

Where the RM-ANOVA indicated a significant interaction, we applied the post hoc Bonferroni test to compare the different groups. Moreover, we applied independent samples t-tests to compare the values obtained in individual ROIs in HS and in the two patient groups. For the network indexes, we applied paired t-tests to compare the values obtained at rest and during motor activation. Correlation analysis was performed to determine the relationship between age or disease duration and the values obtained in the different analyses. Correlations were also evaluated between myoclonus score and CMC or network indexes, removing the effect of age or diseased duration.

Values are expressed as the mean and standard error of the mean. All obtained measures were statistically analyzed using SPSS software (version 17, SPSS Inc. Chicago, IL, USA).

3. Results

For illustrative purposes, [Fig. 1](#) displays four epochs extracted from the EEG-EMG recording performed in two FAME2 (#3 and #11, [Table 1](#)) and two EPM1 patients (#4 and #12, [Table 1](#)) during right-hand extension.

3.1. Spectral analysis at rest

We performed the PSD analysis mainly to exclude different EEG frequency compositions in the two populations of patients, possibly influencing further analysis.

By evaluating the relative PSD values at rest ([Fig. 2](#)), RM-ANOVA showed a significant effect of ROIs in delta ($F(2.11,71.83) = 6.81, p = 0.002$), theta ($F(2.97,100.96) = 6.98, p < 0.001$), alpha ($F(1.51, 51.39) = 16.83p < 0.001$), beta ($F(1.87,63.55) = 7.02, p = 0.002$) bands, but not in the gamma band. Moreover, RM-ANOVA showed a significant interaction ROIs \times GROUPS in delta ($F(2,34) = 21.07, p < 0.001$) and theta ($F(2,34) = 14.91, p < 0.001$) bands, but not in alpha and beta bands.

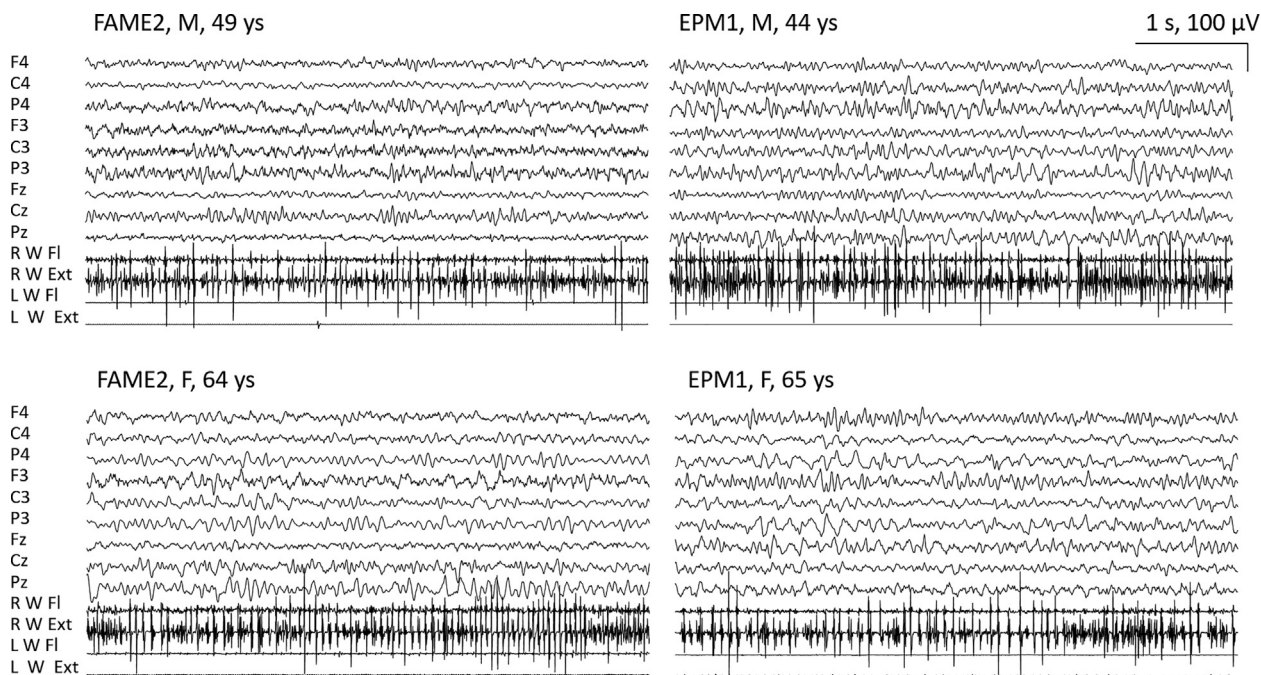


Fig. 1. Five seconds epochs of EEG-EMG recording during active right-hand extension performed in two FAME2 and two EPM1 patients, showing the pattern of action activated myoclonus.

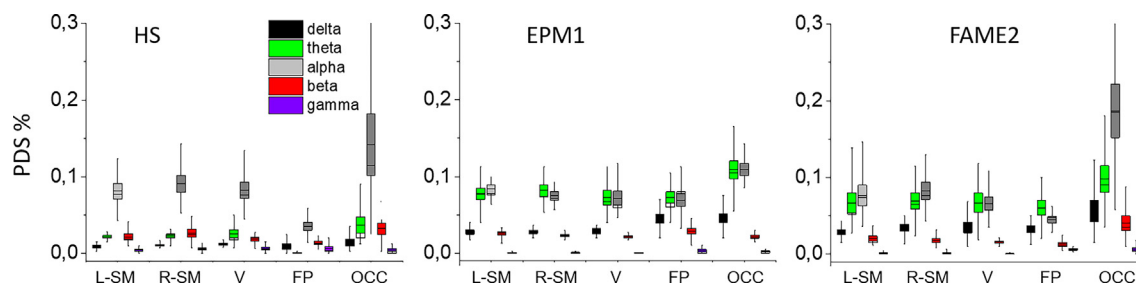


Fig. 2. A: Relative power spectrum density (PSD) measured in healthy subjects (HS), EPM1 and FAME2 patients in different frequency bands and ROIs (regions of interest) L-SM = left sensorimotor, R-SM = right sensorimotor, V = Vertex, FP = bilateral frontopolar, OCC = bilateral occipital). Both FAME2 and EPM1 had higher relative delta power than HS, in all ROIs.

Bonferroni tests indicated significant differences comparing both EPM1 and FAME2 patients with HS with in delta ($p < 0.001$) and theta ($p < 0.001$) bands only, but no differences between the two patient groups.

EPM1 and FAME2 patients, compared to HS, had prominent theta PSD in all ROIs, with the exclusion of the FP ROI.

The spectrum of the EMG signals recorded on wrist muscles during motor activation revealed, on the same epochs selected for CMC analysis, a prominent and sharp peak at a frequency that was similar in FAME2 (mean 19.1 ± 3.4 Hz, range 11.5–23.1 Hz) and EPM1 (mean 19.5 ± 0.4 Hz, range 17.5–23.7 Hz), and multiple and less sharp peaks at higher frequencies. The relative power of the prominent peak was also similar in the two groups (EPM1: mean 0.51 ± 0.04 , range 0.38–0.77; FAME2: mean 0.43 ± 0.03 , range 0.31–0.70).

3.2. Cortico-muscular coherence analysis

The main CMC peak occurred in the beta band at a similar frequency in both EPM1 (mean 18.9 ± 0.2 Hz), and in 12 FAME-2 patients, while occurring in high-alpha frequency in one (#6, 10.2 Hz) (mean 18.7 ± 0.9 Hz). All HS also showed a low but pre-

sent CMC in the beta band (mean 20.4 ± 1.1 Hz). In all groups, the peak was typically prominent in L-SM ROI and often present in V ROI (Fig. 3).

In theta, alpha, and gamma bands, RM-ANOVA did not show main effects. In the beta band, RM-ANOVA showed significant main effects of ROIs ($F(1.71,58.04) = 18.50, p < 0.001$) and GROUPS ($F(2,34) = 7.27, p = 0.002$) and significant interactions ROIs \times GROUPS ($F(3.41,58.04) = 18.50, p = 0.006$). Post-hoc tests revealed that the GROUPS effect was due to EPM1 vs HS ($p = 0.003$) and FAME2 vs HS ($p = 0.018$) without significant differences between the two patient groups (Fig. 3).

Independent samples t-test applied on individual ROIs showed that both FAME2 and EPM1 patients compared to HS, had significantly higher beta CMC in the L-SM ($t(13.8) = 4.4, p < 0.001$ and $t(12.4) = 3.0, p = 0.010$) and V ROIs ($t(12.0) = 3.5, p = 0.002$ and $t(12.1) = 3.6, p = 0.002$), without differences between the two patient groups.

In EPM1, but not in FAME2 patients compared with HS, beta CMC was significantly higher in FP ($t(12.6) = 3.5, p = 0.002$) and in R-SM ($t(12.1) = 3.06, p = 0.010$) ROIs. Similarly, EPM1 had significantly higher values in FP ($t(14.1) = 3.1, p = 0.008$) and R-SM (t

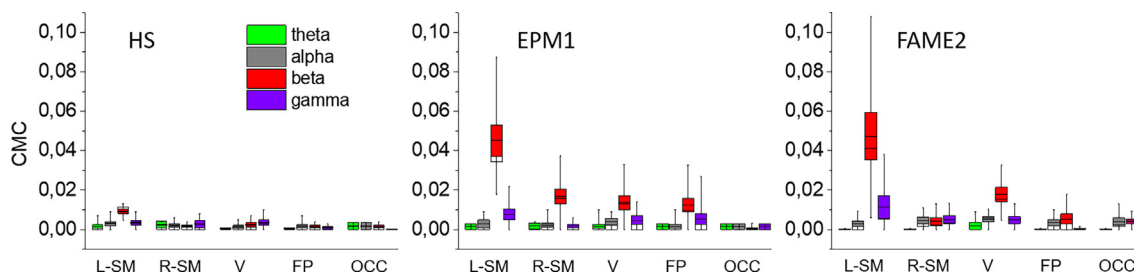


Fig. 3. cortico-muscular coherence (CMC) measured with respect to right wrist extensor in different ROIs during hand extension. Both FAME2 and EPM1 showed significantly higher values in the left sensorimotor (L-SM) and V (=Vertex) ROIs, compared with healthy subjects (HS), while EPM1 had similarly higher CMC values also on R SM and FP ROIs with respect to both HS and FAME2 (**= $p < 0.002$; *= $p < 0.05$). (ROIs = regions of interest: L-SM = left sensorimotor, R-SM = right sensorimotor, V = Vertex, FP = bilateral frontopolar, OCC = bilateral occipital).

(12.6) = 2.8, $p = 0.016$) ROIs also when compared with FAME2 patients.

3.3. Network analysis

3.3.1. Out and In-Degrees

RMANOVA showed a significant effect of ROIs in the alpha band ($F(70.9) = 5.4, p = 0.001$) for Out-degree but not GROUPS effects. For In-degree, RMANOVA did not show any ROIs or GROUPS effects.

3.3.2. Betweenness centrality index

Comparing the two patient groups and HS, statistical analysis showed significant differences only in the beta band. RM-ANOVA showed a significant main effect of ROIs ($F(4,14) = 4.97, p < 0.001$) and GROUPS ($F(2,3) = 12.8, p < 0.001$) and a significant ROIs \times GROUPS interaction ($F(8,136) = 4.21, p < 0.001$) only during motor activation. Post-hoc analysis indicated significant differences between FAME2 and both EPM1 ($p = 0.002$) and HS ($p < 0.001$), but no difference between EPM1 and HS.

Comparing the individual ROIs, t-tests showed that FAME2 patients had, during motor activation, significantly increased BC values in the L-SM ROI compared with both HS ($t(22) = -4.44, p = 0.001$) and EPM1 patients ($t(24) = 5.04, p < 0.001$, Fig. 4A).

During motor activation, in FAME2 patient only, BC values significantly increased in the LSM ROI with respect to those measured at rest (paired t-test: ($t(12) = 5.41, p < 0.001$) (Fig. 4B). In EPM1 patients the behavior was the opposite, with values of BC reduced during muscle activation ($t(12) = -2.80, p = 0.008$). HS did not show a significant difference comparing BC values during motor activation with those measured under resting conditions.

3.3.3. Cluster coefficient

RM-ANOVA on CC values evaluated revealed a significant main effect of GROUPS both in beta ($F(2,34) = 9.47, p < 0.001$) and gamma bands ($F(2,34) = 50.44, p < 0.001$), without ROIs effect.

In the beta band, Bonferroni post hoc tests indicate that the CC values in FAME2 patients were significantly lower than in both HS ($p < 0.001$) and in EPM1 ($p = 0.025$) (Fig. 5A), without significant differences between HS and EPM1 patients.

Even when evaluated on individual ROIs, CC in the beta band showed significantly lower values in FAME2 compared to both HS (t values ranging from 3.4 to 3.7, p values ranging from 0.004 to 0.010) and EPM1 (t values ranging from 3.5 to 5.0, p values ranging from 0.3 to 0.001). EPM1 did not show a significant difference with respect to HS.

In the gamma band, in both FAME2 and EPM1 patients, the CC showed significantly lower values compared to HS (t values ranging from 5.0 to 8.2, p values < 0.001 in all ROIs). When compared with EPM1, FAME2 patients had lower CC in the gamma band in all ROIs (t values ranging from 2.2 to 3.3, p values ranging from 0.032 to 0.005) with the exclusion of the OCC ROI (Fig. 5B).

The comparison between the CC values measured during muscle activation with those measured at rest did not show any significant changes.

3.3.4. Global efficiency and characteristic path length

ANOVA test indicates that EGlob was significantly different between GROUPS in the beta ($F(2,34) = 8.38, p = 0.001$) and the gamma ($F(2,34) = 50.54, p < 0.001$) bands. In both bands, the Bonferroni post-hoc test showed significantly lower EGlob in FAME2 with respect to both HS (beta: $p = 0.002$; gamma: $p < 0.001$) and EPM1 (beta: $p = 0.008$; gamma: $p = 0.008$). In the gamma band,

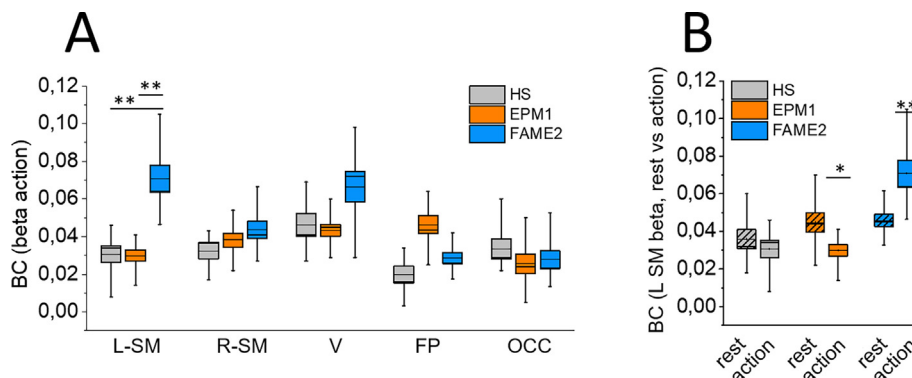


Fig. 4. A: betweenness centrality (BC) measured in the beta-band during right-hand extension in healthy subjects (HS), EPM1 and FAME2 patients in the different ROIs (ROIs = regions of interest: L-SM = left sensorimotor, R-SM = right sensorimotor, V = Vertex, FP = bilateral frontopolar, OCC = bilateral occipital). B: BC values measured on L SM ROI during right-hand extension (action) compared with values measured at rest. Significant differences found comparing action with rest are marked with asterisks (**= $p < 0.001$; *= $p < 0.05$).

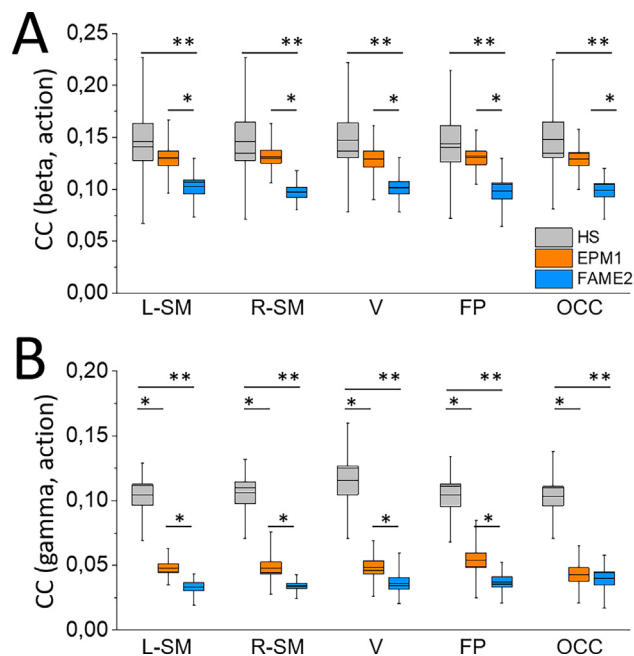


Fig. 5. Clustering Coefficient (CC) measured in beta (A) and gamma (B) bands during right-hand extension in healthy subjects (HS), EPM1 and FAME2 patients in the different ROIs (ROIs = regions of interest: L-SM = left sensorimotor, R-SM = right sensorimotor, V = Vertex, FP = bilateral frontopolar, OCC = bilateral occipital). The differences among subject groups were similar in all ROIs; no significant differences were observed with respect to the same values measured at rest. Significant differences between groups are marked with asterisks (**= $p < 0.001$; *= $p < 0.05$).

FAME2 patients had also lower values compared to EPM1 ($p < 0.001$) (Fig. 6).

CPL showed significant differences between GROUPS in the beta ($F(2,34) = 6.82, p = 0.003$) and gamma ($F(2,34) = 19.30, p < 0.001$) bands. Bonferroni Post-hoc test revealed that CPL had an inverse behavior with respect EGlob. In the beta band, FAME2 patients showed higher CPL values with respect to both HS ($p = 0.006$) and EPM1 patients ($p = 0.016$). In the gamma band, HS had lower values with respect to FAME2 ($p < 0.001$) and EPM1 ($p = 0.013$); moreover, EPM1 had lower values with respect to FAME2 patients ($p = 0.007$).

Both EGlob and CPL measures performed during right-hand movement were not significantly different with respect to those measured at rest.

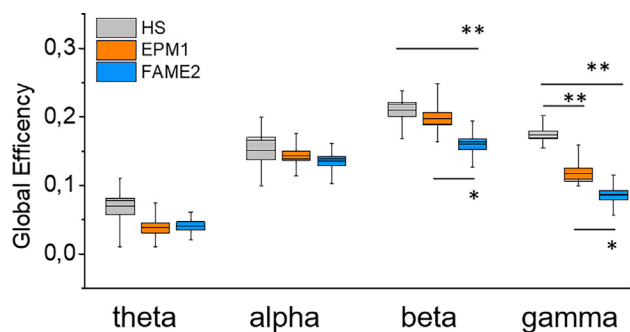


Fig. 6. Global efficiency (EGlob) measured in different frequency bands in healthy subjects (HS), EPM1 and FAME2. The differences among HS and FAME2 patients as well from EPM1 and FAME2 patients were significant in both the beta and gamma bands, while the difference between HS and EPM1 was significant in the gamma band only. Differences are marked with asterisks (**= $p < 0.001$; *= $p < 0.05$).

3.3.5. Associated electrophysiological indexes of enhanced excitability of the sensorimotor cortex.

SEPs evaluated in all EPM1 and in 11 FAME2 patients were defined as “giant” in eight of the patients in each group. The amplitude of N20P25 and of P25N33 was on average higher in EPM1, without a significant difference between EPM1 and FAME2 (N20P25: 16.5 ± 2.3 and $13.8 \pm 2.4 \mu\text{V}$; P25N33: 14.8 ± 4.3 and $13.1 \pm 2.0 \mu\text{V}$). The C-reflex was enhanced at rest in six EPM1 and in eight FAME2 patients.

3.3.6. Correlations

Patient age and disease duration. CMC measured on different ROIs had no significant relationship with age or disease duration. The same occurred for the BC values.

Values of EGlob in the gamma band only negatively correlated with both age ($-0.624(13), p = 0.023$) and disease duration ($-0.641(13), p = 0.018$) in EPM1, but not in FAME2 patients; as well, CPL in gamma band positively correlated with age ($0.666, p = 0.013$) and disease duration ($0.649, p = 0.016$) in gamma band in EPM1 only.

Myoclonus severity score. The obvious difference between the simplified myoclonus score values in EPM1 and FAME2 patients (3.5 ± 0.29 vs $2.0 \pm 0.16, t(18.65) = 4.63, p < 0.001$), and the restricted range of the score values in FAME2, prevented the separate evaluation of the relationship between the myoclonus score and the different evaluated indexes in the two patient populations. However, to test the value of the different indexes with respect to the severity of myoclonus, we grouped the two patient populations. After removing the effect of age, the myoclonus score correlated with the CMC value on R-SM ($0.490(23) p = 0.012$) and FP ($0.511(23), p = 0.009$) ROIs. After removing the effect of disease duration, the myoclonus score correlated with the CMC value on R-SM ($0.424(23) p = 0.034$) and FP ($0.510(23), p = 0.009$) ROIs.

4. Discussion

We examined basic neurophysiological data, including EEG spectral properties at rest and cortico-muscular coherence during segmental motor activation in FAME2 patients presenting with prominent action myoclonus, and we compared the results with those obtained in a group of EPM1 patients, and with a group of healthy subjects.

The spectral properties of the EEG signal revealed an increased amount of slow (theta-delta) frequencies in both EPM1 and FAME2, without significant differences in beta and gamma bands in the two patient groups. This finding can be considered in line with previous observations indicating a trend toward EEG slowing in FAME2 patients (Coppola et al. 2011), and a persistent slowing of background activity in EPM1 (Ferlazzo et al., 2007).

The significant differences that we found comparing FAME2 and EPM1 patients, which could enlighten about the different characteristics and severity of action myoclonus in the two patient groups occurred in beta and gamma bands.

4.1. Parameters expected to influence the severity of myoclonus

An obvious difference was the uneven distribution of CMC in the different cortical regions and the dissimilarities found for the betweenness centrality index. In fact, high CMC in beta frequencies, which is a typical marker of cortically generated myoclonic jerks elicited by segmental motor activation (Silén et al., 2002; Shibasaki 2006; Zutt et al., 2019), characterized the sensorimotor area contralateral to activated hand in both patient groups, but a main difference resided in the more restricted distribution of beta-CMC in FAME2 patients.

Various neurophysiological studies performed in FAME2 patients have highlighted the cortical origin of the myoclonus using the JLBA technique, but only a few have also analyzed the CMC for this purpose (Guerrini et al., 2001, Van Rootselaar et al., 2006). In our study, we evaluated a simple electrode array, grouping the values of electrodes in ROIs; therefore, we did not explore in detail the contribution of specific cortical areas. However, the local setting of high CMC in FAME2 can suggest a less complex “myoclonus” circuitry than in EPM1. The involvement of cortical area exceeding the contralateral motor one in action myoclonus has been repeatedly reported in PME (Hanajima et al., 2001; Panzica et al., 2014), even if its influence on myoclonus severity has been probably not highlighted. Spreading excitation through callosal and cortico-cortical pathways has been originally found (Brown et al., 1991) in patients with cortical myoclonus, and can be a possible mechanism favoring the myoclonus spreading toward additional segments with respect to the activated one.

In previous EEG and MEG studies (Panzica et al., 2014, Franceschetti et al., 2016), comparing EPM1 patients with HS, we already found the presence of high CMC values in regions other than the primary sensorimotor area contralateral to the activated segment in EPM1, and the involvement of the ipsilateral hemisphere. Moreover, in a MEG study, performed to evaluate the changes occurring after drug-induced reduction of the myoclonus severity, we found in EPM1 a significant lessening in the involvement of cortical areas exceeding the contralateral sensorimotor one in the presence of the effective treatment (Franceschetti et al., 2021).

We found another significant difference between FAME2 and EPM1 patients by evaluating the betweenness centrality measured, which is an indicator of the number of shortest paths characterizing the involved local network (García-Prieto et al., 2017), thus describing the ability of the cortical region to maintain high local integration. The significant strengthening of BC, which we found only in FAME2 patients during motor activation with respect to the resting condition, may represent an efficient compensatory phenomenon, completely lost in EPM1, suitable to better execute the movement, and reflecting on the low myoclonus score and the more delimited presentation to the activated muscles observed in these patients. This finding also agrees with what we previously found in a MEG study, indicating an increased BC on motor ROI occurring in EPM1 together with a drug-induced better “control” of action myoclonus (Franceschetti et al., 2021).

Correlation analysis indicated that age and disease duration did not influence the measures found for CMC and betweenness centrality in the two patient populations. The lack of influence of age may depend on the fact that, to evaluate differences with respect to FAME2 we selected adult or aged EPM1 patients, therefore with an age as similar as possible to that of FAME2.

The presence of ASMs in all EPM1, but not in FAME2 patients, may also have reduced the cortical excitability in this population. However, this does not appear to have influenced the persistence of differences in the topography of the CMC, exceeding the primary sensorimotor area in EPM1, and the positive variations of betweenness centrality occurring in FAME2 only, as a possible mechanism suitable to better control action myoclonus.

4.2. Network characteristics

Different information may arise from the evidence of non-local and non-movement-related defects of indexes evaluating the global integration of the network. In FAME2 patients, the clustering coefficient was impaired without any regional prominence, in beta and gamma frequencies, indicating that the degree of local circuitry integration is widely impaired, while in EPM1 patients a similar, although less strong, reduction appears to involve gamma

band only. In line with this, the global efficiency was significantly impaired in both patient groups with respect to healthy subjects, but more strongly impaired in FAME2 patients in beta and gamma bands. Recent data revealed a significant lessening of early high-frequency oscillations in FAME2 patients, suggesting dysfunction of thalamic-somatosensory cortex circuits (Dubbioso et al., 2022). Actually, we found a widespread reduction of fast activities both during active movements and at rest; however, this can be coherent with a significant inability of this disorder in generating fast oscillations, which can be better explored by specific stimulus protocols and waveform analysis.

The generation of beta and gamma activities appeared to be impaired also in EPM1, but more severely in FAME2, compared to both HS and EPM1. In fact, significantly low values were limited to the gamma band in EPM1 showing a negative correlation with age, while in FAME2, low values involved both beta and gamma frequencies and did not correlate with age and disease duration, suggesting that this was an intrinsic feature of this disorder.

Fast activities are mainly generated by subgroups of GABA interneurons (Lewis, 2014), playing a major role in the production of gamma oscillations (Buzsáki and Wang, 2012). Both beta and gamma activities are considered to be generated by the complex network including primary neurons and interneurons (Whittington et al., 2000), so we can consider that the same phenomenon, involving “fast” activities takes place in both patient groups, being more extensive and severe in FAME2.

Gamma oscillations and their network functions are thought to be fundamental for normal cortico-cortical communication, and cognitive functioning (Uhlhaas et al., 2010; Fries 2015). Weakened functional connectivity, evaluated with different algorithms, and mainly involving the frontal, fronto-limbic regions, or the default mode network, has been repeatedly reported in neurodegenerative dementias (Babiloni et al., 2020) and in psychiatric conditions such as depression (Helm et al., 2018) or bipolar disorder (Furlong et al., 2021). We could not evaluate our FAME2 patients with quantitative psychometric tests; therefore, we cannot correlate the observed network impairment with neuropsychological or psychiatric parameters. However, important psychiatric comorbidities have been previously reported in individual patients with FAME2 (Zhang et al., 2020) and tested in family groups (Coppola et al., 2016), with evidence of rather severe neuropsychiatric comorbidity.

The negative relationships between patient age or disease duration and indexes of poor network integration, identified by cluster coefficient and global efficiency in the gamma band, seems to indicate that a poor integrative network ability is associated with the disease progression in EPM1 patients while characterizing the FAME2 patients irrespectively to age and progression.

We have carried out our study in patients with FAME2; therefore, we cannot extend our observations to all patients included in the broad FAME category. However, we think that our findings are significant in the interpretation of the clinical presentation of this specific disorder, with analogies and differences compared to a non-severe form of PME, and they can inspire further evaluations aimed at clarifying its pathophysiology.

5. Limitations and conclusions

The main limits are the limited number of the included subjects, the lack of quantitative measures deriving from neuropsychological evaluation, and the limited definition of the specific cortical areas in the EEG-polygraphic study due to the “standard” EEG recording based on 19 electrodes. Nevertheless, the differences were homogeneous and reached high statistical significance, indicating for FAME2: 1) a better-localized distribution of high beta

CMC values and 2) a clearly increased betweenness centrality index during the active movement possibly influencing the severity of the movement disorder and avoiding the myoclonus spreading outside the activated segment. In both patient groups, compared to HS, there was an obvious decrease in network indexes of local and global network organization, which was however more obvious in FAME2 patients without a clear relationship with the age or disease duration. Further studies could match these finding with neuropsychological deficits in FAME2 population, suggested by previous observation reported literature.

Acknowledgements

We thank Mrs. Alessandra Peirano and Mrs. Paola Anversa for their skillful technical assistance.

Conflict of Interest

None of the authors has potential conflicts of interest to be disclosed.

Funding sources

This research was supported by the Italian Ministry of Health (RC: Ricerca Corrente) not-for-profit sectors.

Author contribution

- 1) Conception and design of the study: Franceschetti S., Visani E.
- 2) Patient selection and clinical assessment: Canafoglia L.
- 3) Data Acquisition: Canafoglia L.
- 4) Software development: Panzica F.
- 5) Analysis and interpretation of data: Franceschetti S., Panzica F., Visani E., Canafoglia L.
- 7) Drafting the article: Franceschetti S., Visani E.
- 7) Data evaluation and discussion: Canafoglia L., Coppola A., Franceschetti S., Striano P.
- 8) Final approval of the manuscript to be submitted: all authors.

References

Babiloni C, Blinowska K, Bonanni L, Cichocki A, De Haan W, Del Percio C, et al. What electrophysiology tells us about Alzheimer's disease: a window into the synchronization and connectivity of brain neurons. *Neurobiol Aging* 2020;85:58–73. <https://doi.org/10.1016/j.neurobiolaging.2019.09.008>

Baccalá LA, de Brito CS, Takahashi DY, Sameshima K. Unified asymptotic theory for all partial directed coherence forms. *Philos Trans A Math Phys Eng Sci* 2013;371(1997):20120158. <https://doi.org/10.1098/rsta.2012.0158>

Brown P, Day BL, Rothwell JC, Thompson PD, Marsden CD. Intrahemispheric and interhemispheric spread of cerebral cortical myoclonic activity and its relevance to epilepsy. *Brain* 1991;114:2333–51. <https://doi.org/10.1093/brain/114.5.2333>

Buzsáki G, Wang XJ. Mechanisms of gamma oscillations. *Annu Rev Neurosci* 2012;35:203–25. <https://doi.org/10.1146/annurev-neuro-062111-150444>

Canafoglia L, Ferlazzo E, Michelucci R, Striano P, Magaouda A, Gambardella A, et al. Variable course of Unverricht-Lundborg disease: Early prognostic factors. *Neurology* 2017;89(16):1691–7. <https://doi.org/10.1212/WNL.0000000000004518>

Cen Z, Huang C, Yin H, Ding X, Xie F, Lu X, et al. Clinical and neurophysiological features of familial cortical myoclonic tremor with epilepsy. *Mov Disord* 2016;31:1704–10. <https://doi.org/10.1002/mds.26756>

Coppola A, Caccavale C, Santulli L, Balestrini S, Cagnetti C, Licchetta L, et al. Psychiatric comorbidities in patients from seven families with autosomal dominant cortical tremor, myoclonus, and epilepsy. *Epilepsy Behav* 2016;56:38–43. <https://doi.org/10.1016/j.yebeh.2015.12.038> PMID: 26827300.

Coppola A, Santulli L, Del Gaudio L, Minetti C, Striano S, Zara F, Striano P. Natural history and long-term evolution in families with autosomal dominant cortical tremor, myoclonus, and epilepsy. *Epilepsia* 2011;52(7):1245–50. <https://doi.org/10.1111/j.1528-1167.2011.03017.x>

Corbett MA, Kroes T, Veneziano L, Bennett MF, Florian R, Schneider AL, et al. Intronic ATTTC repeat expansions in STARD7 in familial adult myoclonic epilepsy linked

to chromosome 2. *Nat Commun* 2019;10:4920. <https://doi.org/10.1038/s41467-019-12671-y>

Crompton DE, Sadleir LG, Bromhead CJ, Bahlo M, Bellows ST, Arsov T, et al. Familial adult myoclonic epilepsy: recognition of mild phenotypes and refinement of the 2q locus. *Arch Neurol* 2012;69(4):474–81. <https://doi.org/10.1001/archneurol.2011.584>

Dubbioso R, Striano P, Tomasevic L, Bilo L, Esposito M, Manganeli F, Coppola A. Abnormal sensorimotor cortex and thalamo-cortical networks in familial adult myoclonic epilepsy type 2: pathophysiology and diagnostic implications. *Brain Commun* 2022;4(1):fcac037. <https://doi.org/10.1093/braincomms/fcac037>

Ferlazzo E, Magaouda A, Striano P, Vi-Hong N, Serra S, Genton P. Long-term evolution of EEG in Unverricht-Lundborg disease. *Epilepsy Res* 2007;73(3):219–27. <https://doi.org/10.1016/j.eplepsyres.2006.10.006>

Florian RT, Kraft F, Leitão E, Kaya S, Klebe S, Magnin E, et al. Unstable TTTTA/TTTCA expansions in MARCH6 are associated with Familial Adult Myoclonic Epilepsy type 3. *Nat Commun* 2019;10(1):4919. <https://doi.org/10.1038/s41467-019-12763-9>

Franceschetti S, Canafoglia L, Rotondi F, Visani E, Granvillano A, Panzica F. The network sustaining action myoclonus: a MEG-EMG study in patients with EPM1. *BMC Neurol* 2016;16(1):214. <https://doi.org/10.1186/s12883-016-0738-5>

Franceschetti S, Visani E, Rossi Sebastiano D, Duran D, Granata T, Solazzi R, et al. Cortico-muscular and cortico-cortical coherence changes resulting from Perampanel treatment in patients with cortical myoclonus. *Clin Neurophysiol* 2021;132:1057–63. <https://doi.org/10.1016/j.clinph.2021.01.018>

Fries P. Rhythms for Cognition: Communication through Coherence. *Neuron* 2015;88(1):220–35. <https://doi.org/10.1016/j.neuron.2015.09.034>

Furlong LS, Rossell SL, Caruana GF, Cropley VL, Hughes M, Van Rheenen TE. The activity and connectivity of the facial emotion processing neural circuitry in bipolar disorder: a systematic review. *J Affect Disord* 2021;279:518–48. <https://doi.org/10.1016/j.jad.2020.10.038>

García-Prieto J, Bajo R, Pereda E. Efficient Computation of Functional Brain Networks: toward Real-Time Functional Connectivity. *Front Neuroinform* 2017;11:8. <https://doi.org/10.3389/fninf.2017.00008>

Guerrini R, Bonanni P, Patrignani A, Brown P, Parmeggiani L, Grosse P, et al. Autosomal dominant cortical myoclonus and epilepsy (ADCME) with complex partial and generalized seizures: A newly recognized epilepsy syndrome with linkage to chromosome 2p11.1-q12.2. *Brain* 2001;124:2459–75. <https://doi.org/10.1093/brain/124.12.2459>

Hanajima R, Ugawa Y, Okabe S, Yuasa K, Shiio Y, Iwata NK, Kanazawa I. Interhemispheric interaction between the hand motor areas in patients with cortical myoclonus. *Clin Neurophysiol* 2001;112(4):623–6. [https://doi.org/10.1016/s1388-2457\(01\)00477-1](https://doi.org/10.1016/s1388-2457(01)00477-1)

Helm K, Viol K, Weiger TM, Tass PA, Grefkes C, Del Monte D, Schiepek G. Neuronal connectivity in major depressive disorder: a systematic review. *Neuropsychiatr Dis Treat* 2018;14:2715–37. <https://doi.org/10.2147/NDT.S170989>

Ikeda A, Kakigi R, Funai N, Neshige R, Kuroda Y, Shibasaki H. Cortical tremor: a variant of cortical reflex myoclonus. *Neurology* 1990;40(10):1561–5. <https://doi.org/10.1212/wnl.40.10.1561>

Ishihara H, Doi K, Mitsui J, Yoshimura J, Matsukawa MK, Fujiyama A, et al. Expansions of intronic TTTCA and TTTTA repeats in benign adult familial myoclonic epilepsy. *Nat Genet* 2018;50(4):581–90. <https://doi.org/10.1038/s41588-018-0067-2>

Kälviäinen R, Khyuppenen J, Koskenkorva P, Eriksson K, Vanninen R, Mervaala E. Clinical picture of EPM1-Unverricht-Lundborg disease. *Epilepsia* 2008;49(4):549–56. <https://doi.org/10.1111/j.1528-1167.2008.01546.x> PMID: 18325013.

Kobayashi K, Hitomi T, Matsumoto R, Watanabe M, Takahashi R, Ikeda A. Nationwide survey in Japan endorsed diagnostic criteria of benign adult familial myoclonic epilepsy. *Seizure* 2018;61:14–22. <https://doi.org/10.1016/j.seizure.2018.07.014>

Latorre A, Rocchi L, Magrinelli F, Mulroy E, Berardelli A, Rothwell JC, Bhatia KP. Unraveling the enigma of cortical tremor and other forms of cortical myoclonus. *Brain* 2020;143(9):2653–63. <https://doi.org/10.1093/brain/awaa129>

Lewis DA. Inhibitory neurons in human cortical circuits: substrate for cognitive dysfunction in schizophrenia. *Curr Opin Neurobiol* 2014;26:22–6. <https://doi.org/10.1016/j.conb.2013.11.003>

Licchetta L, Pippucci T, Bisulli F, Cantalupo G, Magini P, Alvisi L, et al. A novel pedigree with familial cortical myoclonic tremor and epilepsy (FCMTE): clinical characterization, refinement of the FCMTE2 locus, and confirmation of a founder haplotype. *Epilepsia* 2013;54(7):1298–306. <https://doi.org/10.1111/epi.12216>

Magaouda A, Gelisse P, Genton P. Antimyoclonic effect of levetiracetam in 13 patients with Unverricht-Lundborg disease: clinical observations. *Epilepsia* 2004;45(6):678–81. <https://doi.org/10.1111/j.0013-9580.2004.56902.x>

Ogumi E, Hayashi A, Ishii A, Mizusawa H, Shoji S. A case of cortical tremor as a variant of cortical reflex myoclonus. *Eur Neurol* 1995;35(1):63–4. <https://doi.org/10.1159/000117093>

Panzica F, Canafoglia L, Franceschetti S, Binelli S, Ciano C, Visani E, Avanzini G. Movement-activated myoclonus in genetically defined progressive myoclonic epilepsies: EEG-EMG relationship estimated using autoregressive models. *Clin Neurophysiol* 2003;114(6):1041–52. [https://doi.org/10.1016/s1388-2457\(03\)00066-x](https://doi.org/10.1016/s1388-2457(03)00066-x)

Panzica F, Canafoglia L, Franceschetti S. EEG-EMG information flow in movement-activated myoclonus in patients with Unverricht-Lundborg disease. *Clin*

- Neurophysiol 2014;125(9):1803–8. <https://doi.org/10.1016/j.clinph.2014.01.005>.
- Ramachandran N, Girard JM, Turnbull J, Minassian BA. The autosomal recessively inherited progressive myoclonus epilepsies and their genes. *Epilepsia*. 2009;50 (Suppl 5):29–36. <https://doi.org/10.1111/j.1528-1167.2009.02117.x>. PMID: 19469843.
- Schneider T, Neumaier A. Algorithm 808: ARfit – A Matlab package for the estimation of parameters and eigenmodes of multivariate autoregressive models. *ACM Trans. Math. Softw* 2001;27:58–65.
- Shibasaki H. Neurophysiological classification of myoclonus. *Neurophysiol Clin* 2006;36(5–6):267–9. <https://doi.org/10.1016/j.neucli.2006.11.004>.
- Silén T, Forss N, Salenius S, Karjalainen T, Hari R. Oscillatory cortical drive to isometrically contracting muscle in Unverricht-Lundborg type progressive myoclonus epilepsy (ULD). *Clin Neurophysiol* 2002;113(12):1973–9. [https://doi.org/10.1016/s1388-2457\(02\)00196-7](https://doi.org/10.1016/s1388-2457(02)00196-7).
- Terada K, Ikeda A, Mima T, Kimura M, Nagahama Y, Kamioka Y, et al. Familial cortical myoclonic tremor as a unique form of cortical reflex myoclonus. *Mov Disord* 1997;12(3):370–7. <https://doi.org/10.1002/mds.870120316>.
- Theiler J, Eubank S, Longtin A, Galdrikian B, Farmer JD. Testing for non-linearity in time series: the method of surrogate data. *Physica D* 1992;58(1–4):77–94.
- Tojima M, Hitomi T, Matsuhashi M, Neshige S, Usami K, Oi K, et al. A biomarker for benign adult familial Myoclonus epilepsy: High-frequency activities in giant somatosensory evoked potentials. *Mov Disord* 2021;36(10):2335–45. <https://doi.org/10.1002/mds.28666>.
- Uhlhaas PJ, Singer W. Abnormal neural oscillations and synchrony in schizophrenia. *Nat Rev Neurosci* 2010;11(2):100–13. <https://doi.org/10.1038/nrn2774>.
- van Rootselaar AF, Maurits NM, Koelman JH, van der Hoeven JH, Bour LJ, Leenders KL, et al. Coherence analysis differentiates between cortical myoclonic tremor and essential tremor. *Mov Disord* 2006;21(2):215–22. <https://doi.org/10.1002/mds.20703>.
- Vidaurre C, Sander TH, Schlögl A. BioSig: the free and open source software library for biomedical signal processing. *Comput Intell Neurosci*. 2011;2011. <https://doi.org/10.1155/2011/935364>. 935364.
- Visani E, Canafoglia L, Rossi Sebastiano D, Agazzi P, Panzica F, Scaiola V, Ciano C, Franceschetti S. Giant SEPs and SEP-recovery function in Unverricht-Lundborg disease. *Clin Neurophysiol*. 2013;124(5):1013–8. <https://doi.org/10.1016/j.clinph.2012.11.011>. PMID: 23276489.
- Wang G, Song Y, Su J, Fan Z, Xu L, Fang P, et al. Altered cerebellar-motor loop in benign adult familial myoclonic epilepsy type 1: The structural basis of cortical tremor. *Epilepsia* 2022;63(12):3192–203. <https://doi.org/10.1111/epi.17430>.
- Whittington MA, Traub RD, Kopell N, Ermentrout B, Buhl EH. Inhibition-based rhythms: experimental and mathematical observations on network dynamics. *Int J Psychophysiol* 2000;38(3):315–36. [https://doi.org/10.1016/s0167-8760\(00\)00173-2](https://doi.org/10.1016/s0167-8760(00)00173-2).
- Yeetong P, Pongpanich M, Srichomthong C, Assawapitaksakul A, Shotelersuk V, Tantirukdham N, et al. TTCA repeat insertions in an intron of YEATS2 in benign adult familial myoclonic epilepsy type 4. *Brain* 2019;142(11):3360–6. <https://doi.org/10.1093/brain/awz267>.
- Zhang Y, Xiong W, Lu L, Zhou D. Familial cortical myoclonic tremor with epilepsy: TTTCA/TTTTA repeat expansions and expanding phenotype in two Chinese families. *Brain Res* 2020;1737. <https://doi.org/10.1016/j.brainres.2020.146796>. 146796.
- Zoubir A, Iskander DR. Bootstrap techniques for signal processing. Cambridge University Press 2004. <https://doi.org/10.1017/CBO9780511536717>.
- Zutt R, Elting JW, Tijssen MAJ. Tremor and myoclonus. *Handb Clin Neurol* 2019;161:149–65. <https://doi.org/10.1016/B978-0-444-64142-7.00046-1>.